Formation, growth and evaporation of heterogeneous dust grains in oxygen–rich environments under oscillating thermodynamic conditions

Kyung Sook Jeong, Jan Martin Winters, Axel J. Fleischer, and Erwin Sedlmayr

Institut für Astronomie und Astrophysik, Technische Universität Berlin, Sekr. PN 8-1, Hardenbergstr. 36, D-10623 Berlin, FRG

1 Introduction

In order to understand the physical processes determining the dynamical structure and behaviour of circumstellar dust shells (CDS) around long–period variables (LPVs), it is inevitable to take consistently into account the complex interplay among dust formation, hydrodynamics, chemistry, and thermodynamics. Since the dust component, due to its huge absorption cross section with respect to the stellar radiation field, plays a decisive role for the structure and dynamics of the circumstellar shell, a proper description of formation and growth of the dust grains is a necessary prerequisite to model the CDS around LPVs.

In contrast to the carbon–rich situation, where mainly *homogeneous* amorphous carbon grains are formed (Fleischer et al., 1992), in an oxygen–rich environment almost all carbon is locked up in the chemically inert CO molecule. Therefore, the grains only can be formed from molecules containing the remaining oxygen and the less abundant elements Mg, Si, S, Fe, Al. In this case a *heterogeneous* element composition of the emerging dust component has to be expected.

To focus the investigation on the heterogeneous condensation of these elements, in this poster we consider two gas elements which are subject to periodic variations of temperature and density in order to simulate the varying conditions encountered by gas elements moving through the circumstellar shell of an oxygen–rich LPV. Assuming chemical equilibrium in the gas phase, we describe the nucleation process of the seed particles according to the equations given in Gail et al. (1984). The seed nuclei of these particles (homogeneous SiO and Fe clusters, cf. Gail & Sedlmayr (1986)) grow by addition of those molecular species which have a stable solid phase under the local thermodynamic conditions prevailing in the circumstellar environment. Heterogeneous growth of the particles is treated by means of a moment method (Dominik et al. 1993), while grain evaporation is described by the formalism developed in Gauger et al. (1990).

2 Modeling method

- We consider an **adiabatic gas element** with a prescribed sinusoidal temporal variation of the temperature. Correspondingly, also the density varies sinusoidally in time. The values of the period P, the mean temperature $\bar{T}$, the temperature amplitude ΔT, and the mean density $\bar{\rho}$ as well as the value of the adiabatic exponent γ are given in Tab. 1.

- Two cases are calculated:

  A) constant temperature amplitude

  B) damped temperature amplitude

- Under these two thermal scenarios, nucleation of seed particles, heterogeneous growth, and thermal evaporation of dust grains is investigated in an oxygen–rich environment.

- Nucleation of homogeneous Fe–clusters as seed nuclei is considered. For details see Gail et al. (1984) and Gail & Sedlmayr (1986).

- Heterogeneous growth of these particles is treated by the formalism given in Dominik et al. (1993).

- Thermal evaporation of dust particles is calculated according to the method developed by Gauger et al. (1990).

Table 1: Parameters for the calculation

P [d]	$\bar{T}$ [K]	ΔT [K]	$\bar{\rho}$ [g cm^{-3}]	γ
300	1100	700	10^{-13}	5/3

3 Results

Case A

- Nucleation of Fe starts around $T = 920\,$K, with a maximum nucleation rate around $T = 690\,$K; see Fig. 1.

- The different species successively contribute to grain growth (cf. upper diagram of Fig. 3), according to a stability hierarchy established by the thermodynamic conditions. The last element contributing to growth is **sulphur**.

- Growth of particles up to an average size of approx. $7 * 10^{-3}\mu$m.

- All dust–forming elements, with the exception of oxygen, become completely depleted from the gas phase (cf. Figs. 2, 3 and 7).

- Evaporation of S around $T = 680\,\mathrm{K}$, of Fe around $T = 1200\,\mathrm{K}$, and of Si around $T = 1360\,\mathrm{K}$. Complete destruction of grains at $T = 1600\,\mathrm{K}$ (cf. lower panel of Fig. 3). After evaporation of Fe in the grain mantle at $T = 1200\,\mathrm{K}$, the Fe core is still stable up to $T = 1600\,\mathrm{K}$, since it is surrounded by the very stable aluminium bearing molecules.
- the destruction of the cores occurs in a very narrow range of temperature.

Case B

- Phase of nucleation and growth similar to Case A. (cf. Fig.4).
- Caused by the higher density, the mean particle radius becomes larger (cf. Fig. 4).
- Evaporation of S bearing molecules, but **no complete destruction of grains** (cf. Fig. 4 and lower panel of Fig. 6).

Acknowledgements: This work has been supported by the Deutsche Forschungsgemeinschaft (grant Se 420/8–1), Bundesministerium für Bildung und Forschung (grant 05 3BT13A 6) and the FAZIT Stiftung. The calculations were performed on the CRAY computers of the ZIB (Berlin).

References

Dominik, C., Sedlmayr, E., and Gail, H.-P., 1993. Dust formation in stellar winds. VI. Moment equations for the formation of heterogeneous and core-mantle grains. *A&A*, **277**, 578–594.
Fleischer, A. J., Gauger, A., and Sedlmayr, E., 1992. Circumstellar Dust shells around Long-period Variables. I. Dynamical models of C-stars including dust formation, growth and evaporation. *A&A*, **266**, 321–339.
Gail, H.-P. and Sedlmayr, E., 1986. The primary condensation process for dust around late M-type stars. *A&A*, **166**, 225–236.
Gail, H.-P., Keller, R., and Sedlmayr, E., 1984. Dust formation in stellar winds. I. A rapid computational method and application to graphite condensation. *A&A*, **133**, 320–332.
Gauger, A., Gail, H.-P., and Sedlmayr, E., 1990. Dust formation, growth and evaporation in a cool pulsating circumstellar shell. *A&A*, **235**, 345–361.

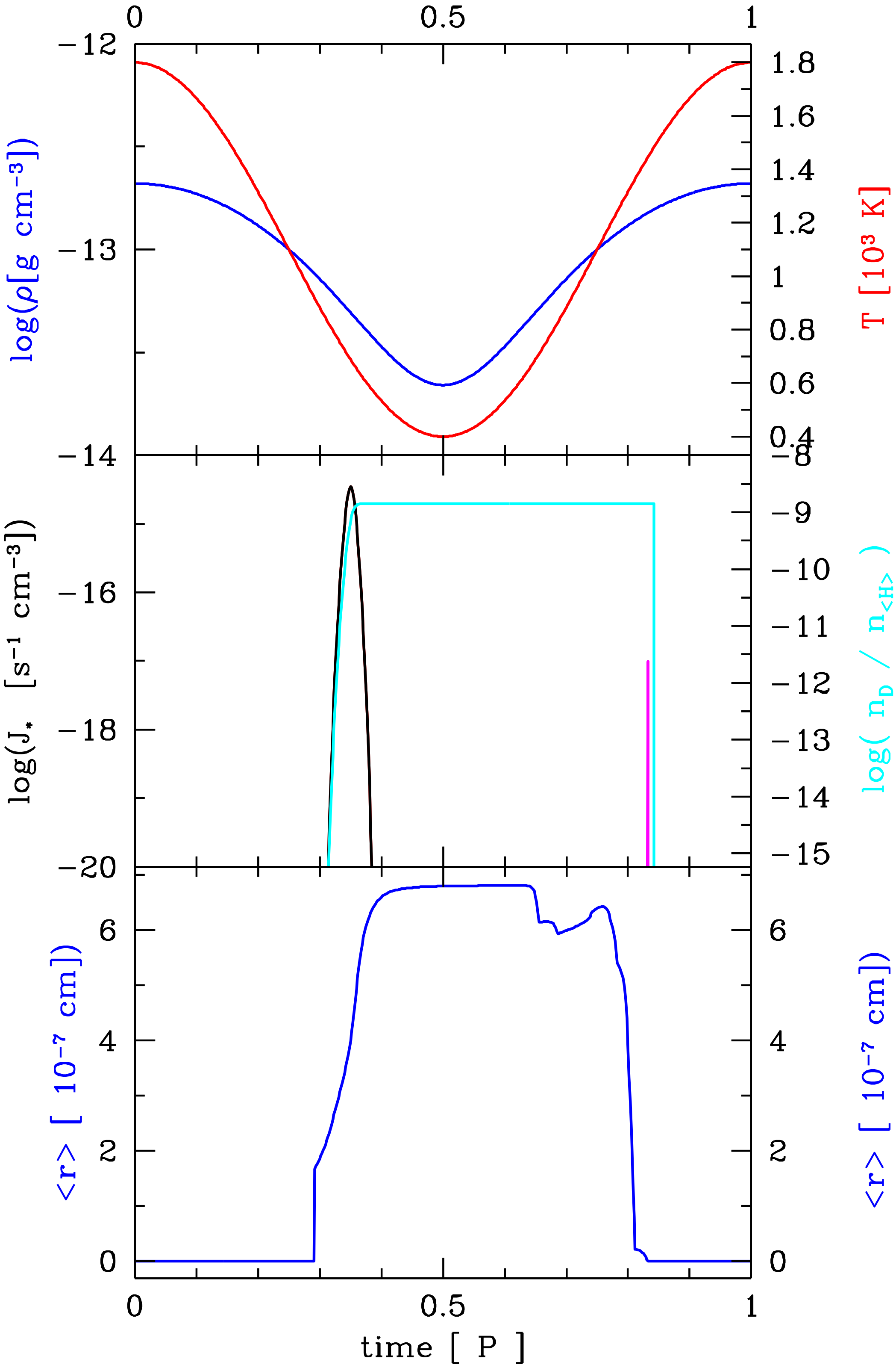

Figure 1: Thermodynamical and dust quantities for Case A.
upper diagram: Logarithm of the mass density ρ (blue line, l.h.s. ordinate) and Temperature T (red line, r.h.s. ordinate); **middle diagram:** Logarithm of the nucleation and evaporation rate J_* and $J_{\rm ev}$ ($J_{*,\rm Fe}$: black line, $J_{\rm ev}$ red line, l.h.s. ordinate) and logarithm of the number of dust particles per H–atom $n_{\rm D}/n_{<\rm H>}$ (blue line, r.h.s. ordinate); **lower diagram:** mean particle radius $<$ r $>$.

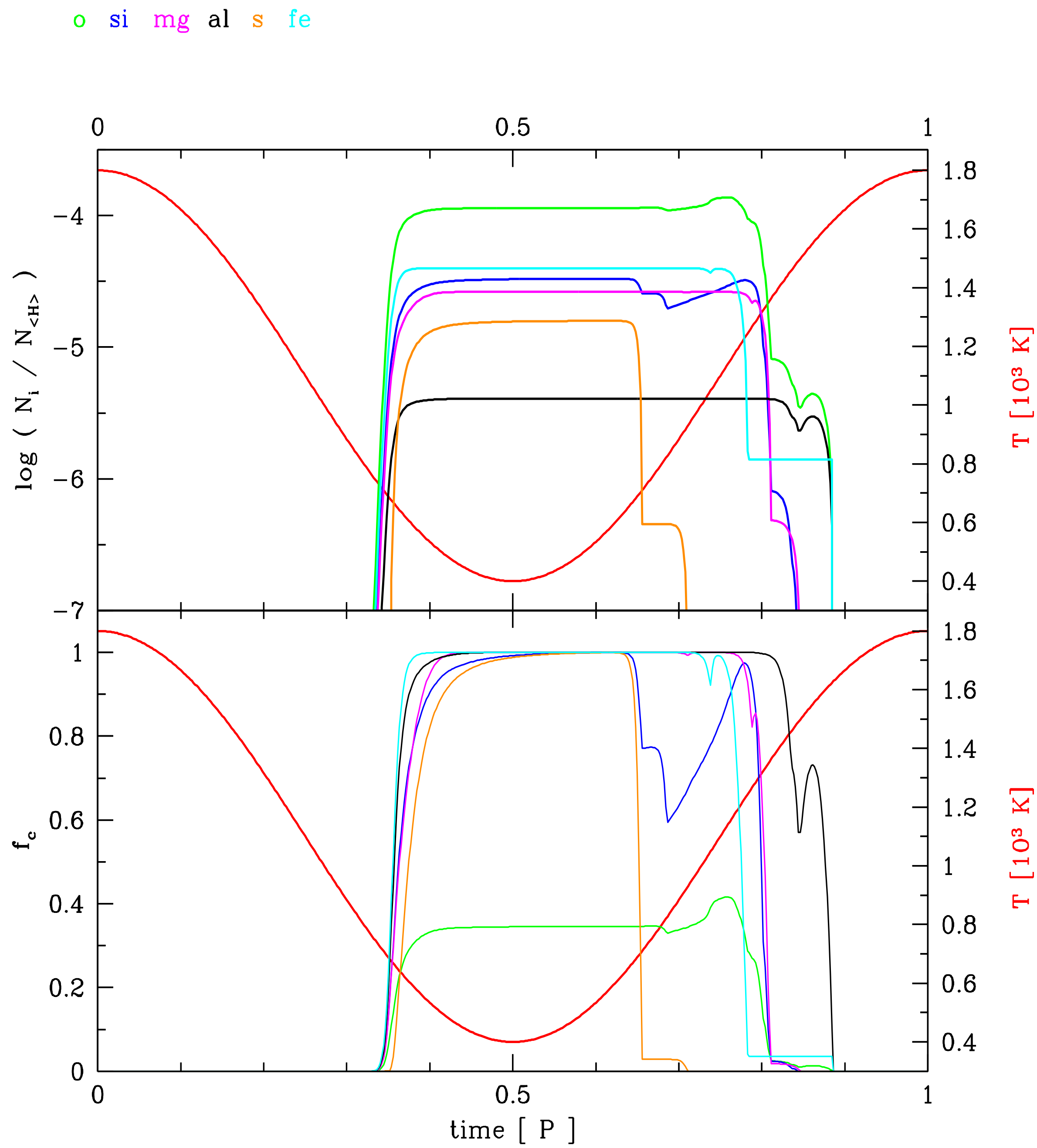

Figure 2: Chemical composition of the dust grains as a function of time for Case A.

upper diagram: Logarithm of the number of condensed atoms of element i per H–atom $n_i/n_{<\mathrm{H}>}$,

lower diagram: Degree of condensation f_c of the elements.

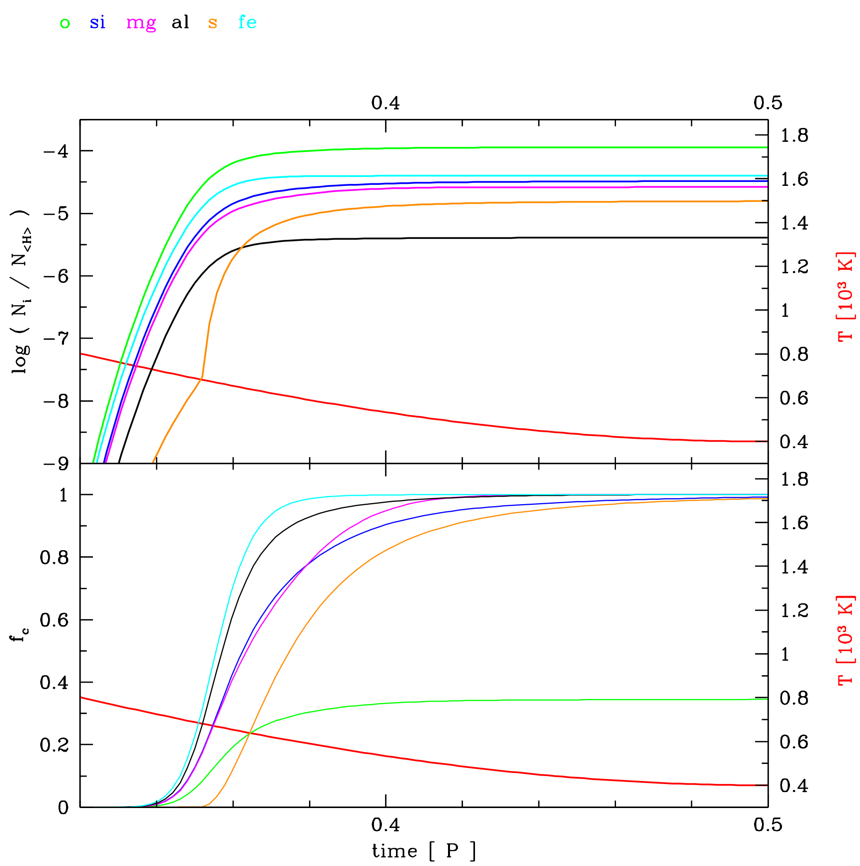

Figure 3: Cut of Fig. 2 for the time interval of grain growth (**upper figure**) and for the time interval of evaporation (**lower figure**)

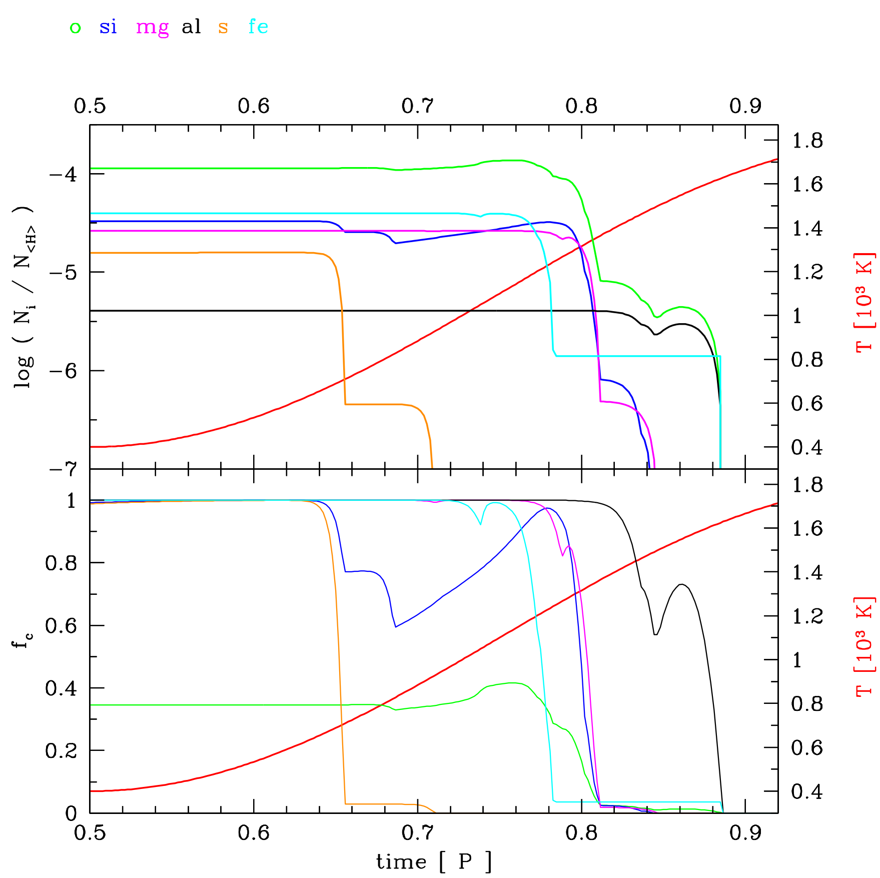

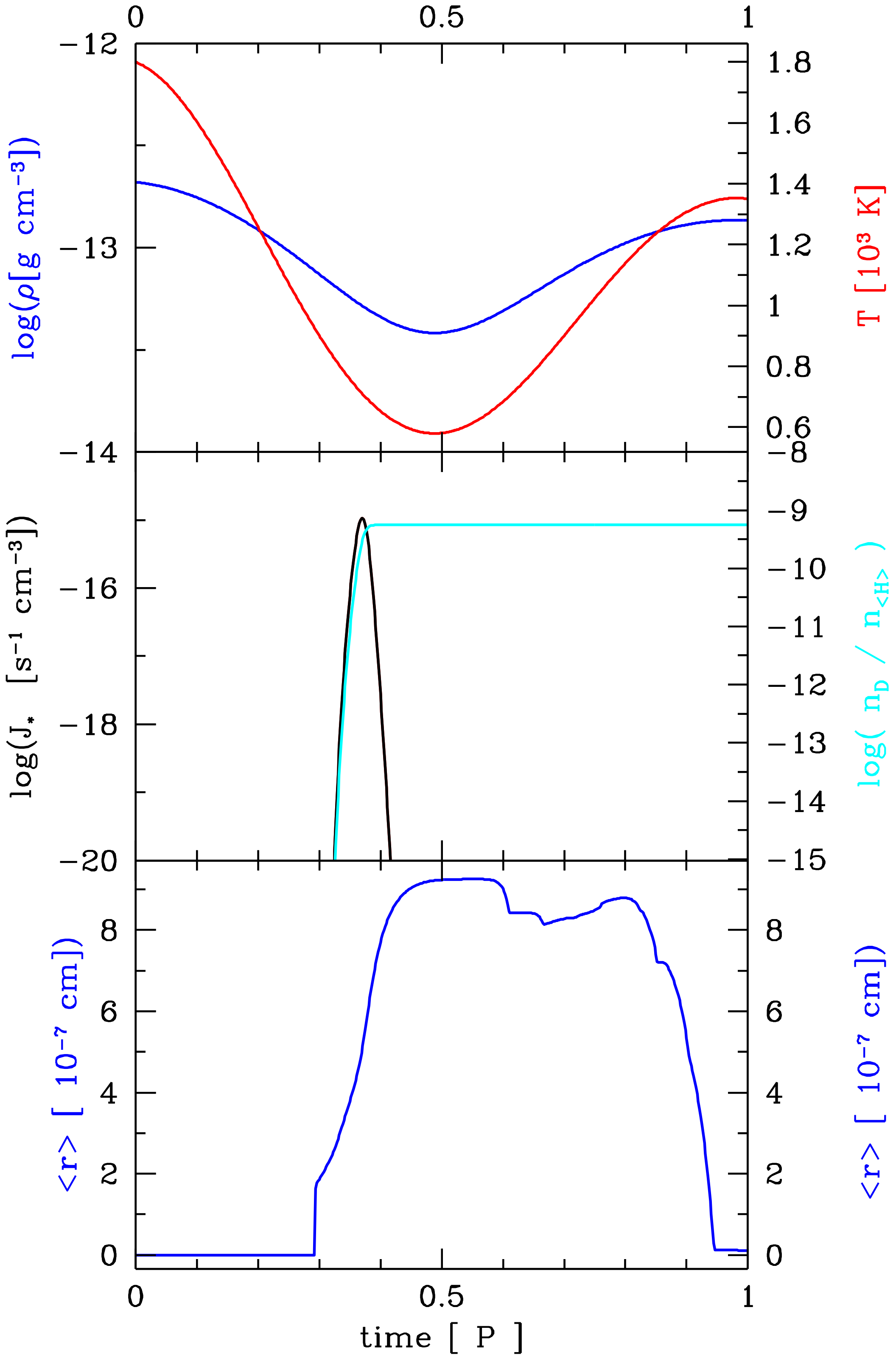

Figure 4: Thermodynamical and dust quantities for Case B.
upper diagram: Logarithm of the mass density ρ (blue line, l.h.s. ordinate) and Temperature T (red line, r.h.s. ordinate); **middle diagram:** Logarithm of the nucleation and evaporation rate J_* and $J_{\rm ev}$ ($J_{*,\rm Fe}$: black line, $J_{\rm ev}$ red line, l.h.s. ordinate) and logarithm of the number of dust particles per H–atom $n_{\rm D}/n_{<\rm H>}$ (blue line, r.h.s. ordinate); **lower diagram:** mean particle radius $< {\rm r} >$.

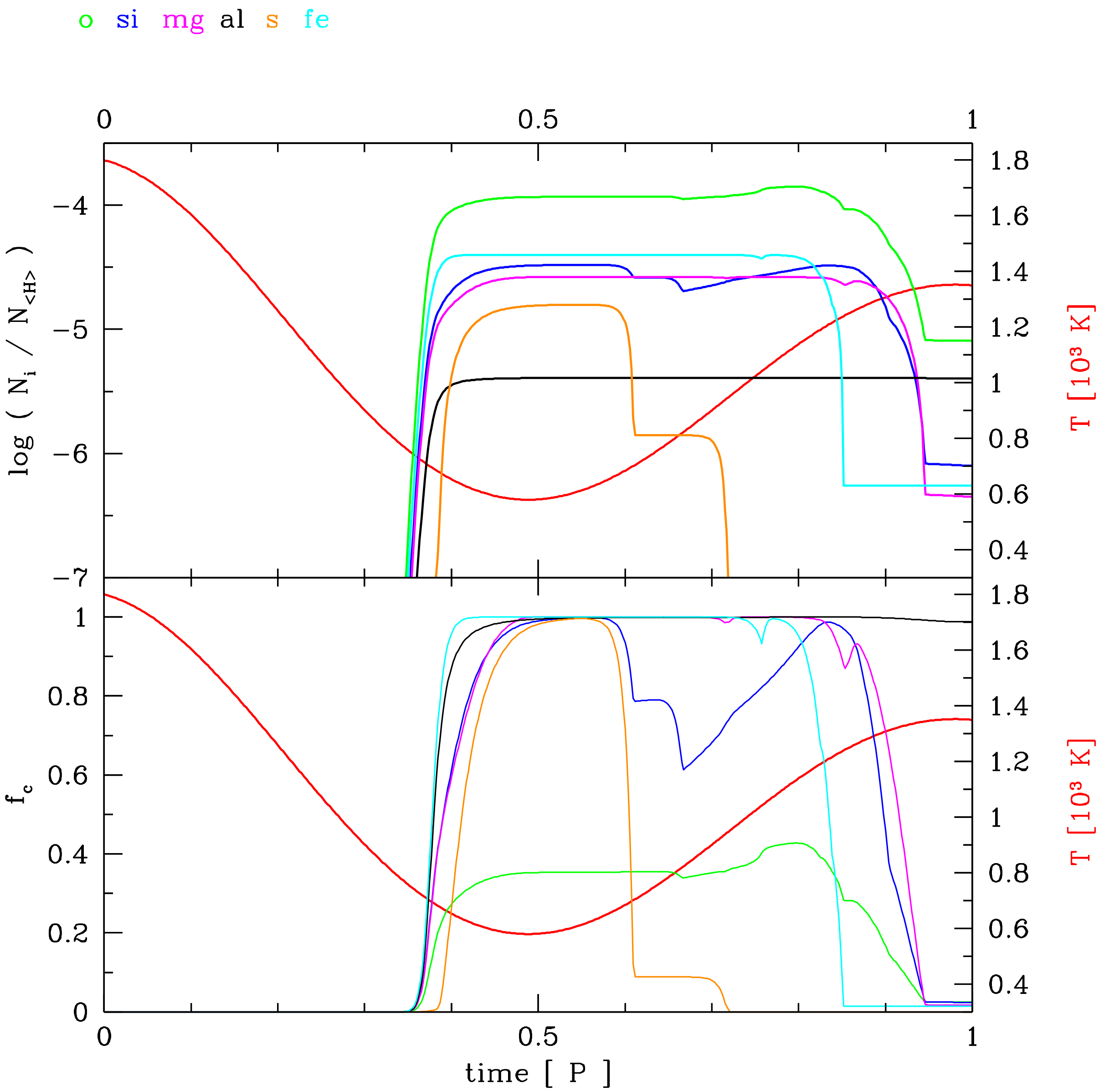

Figure 5: Chemical composition of the dust grains as a function of time for Case B.
upper diagram: Logarithm of the number of condensed atoms of element i per H–atom $n_i/n_{<\mathrm{H}>}$,
lower diagram: Degree of condensation f_c of the elements.

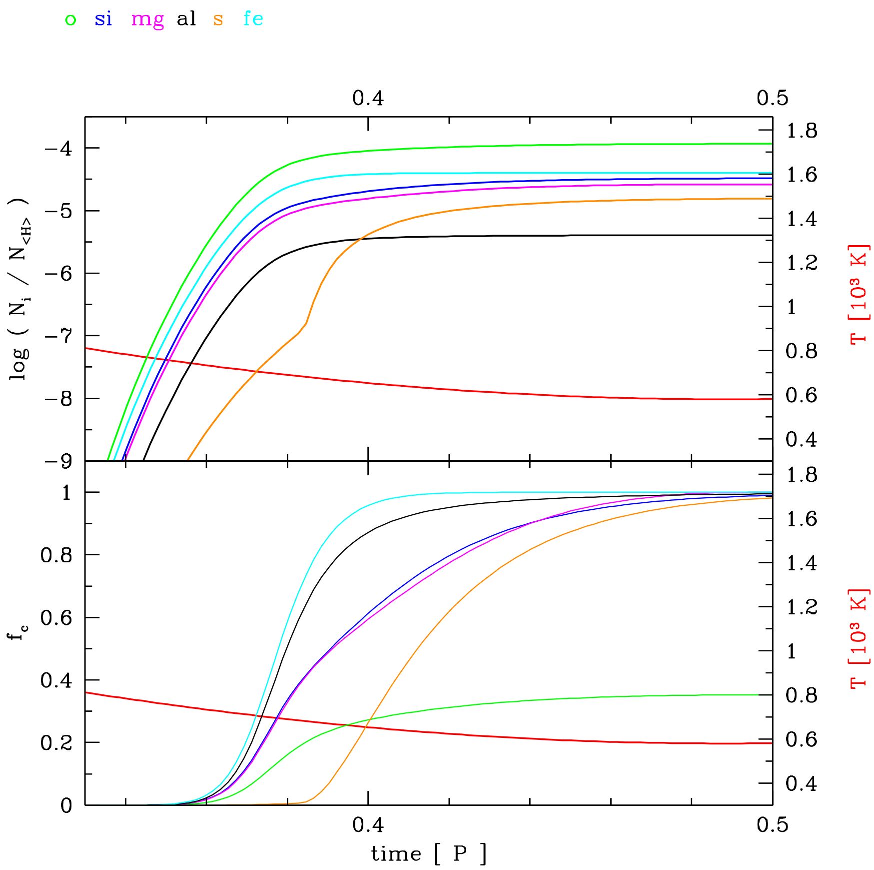

Figure 6: Cut of Fig. 5 for the time interval of grain growth (**upper figure**) and for the time interval of evaporation (**lower figure**)

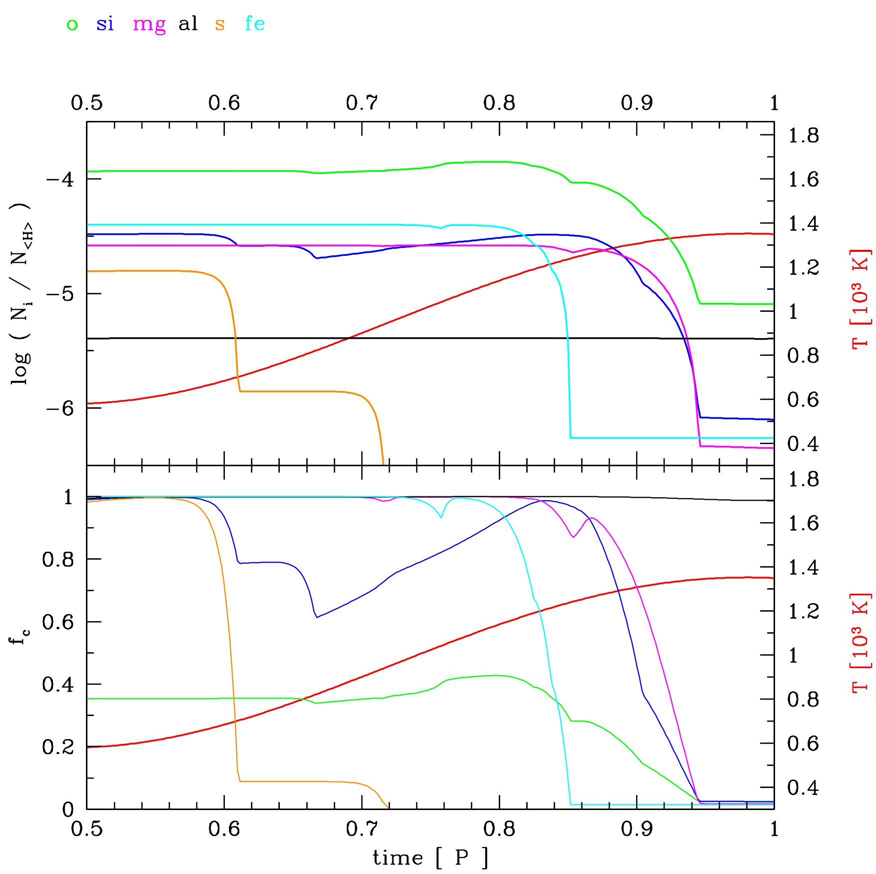

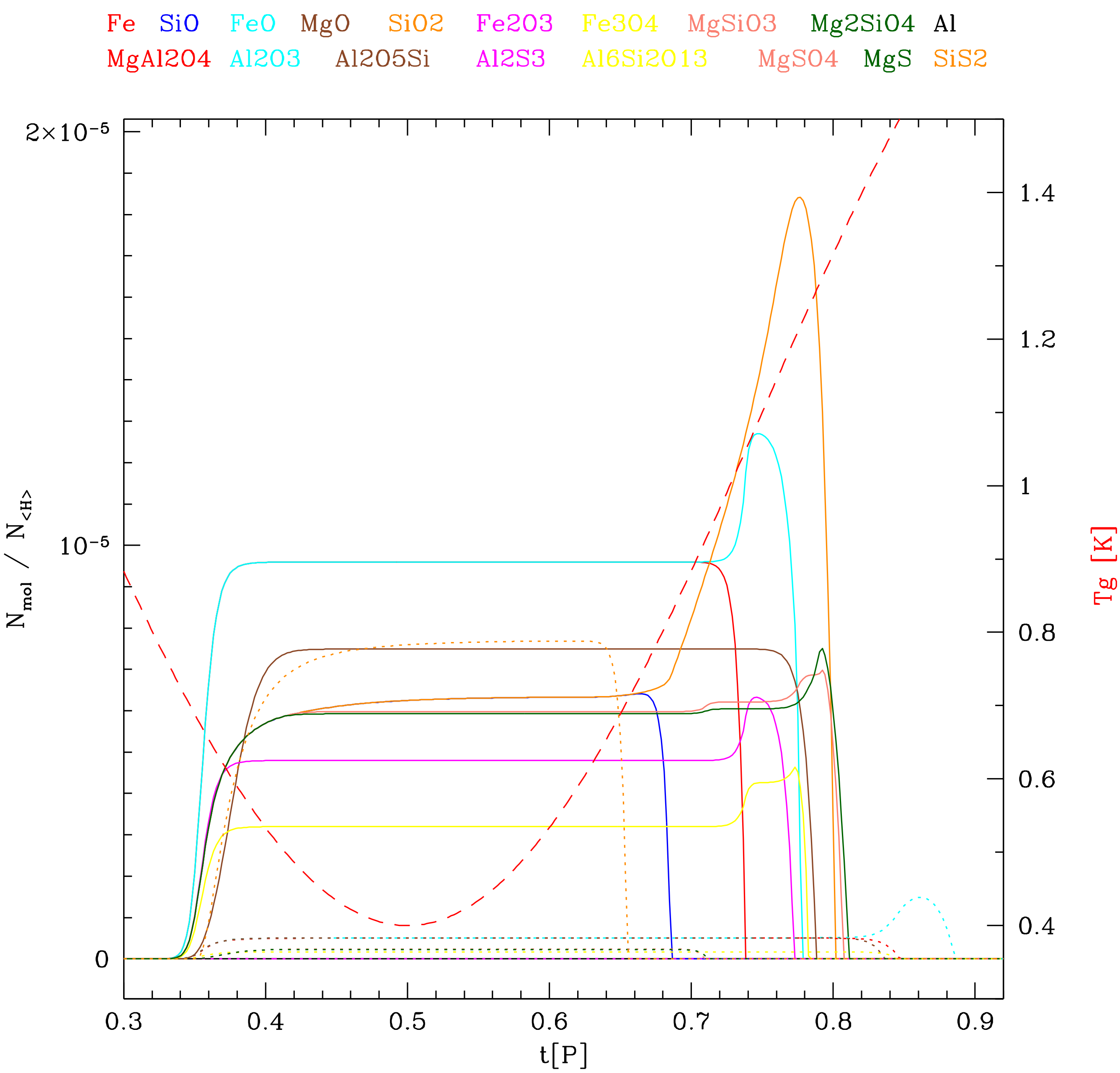

Figure 7: Molecular composition of the dust grains for **case A**

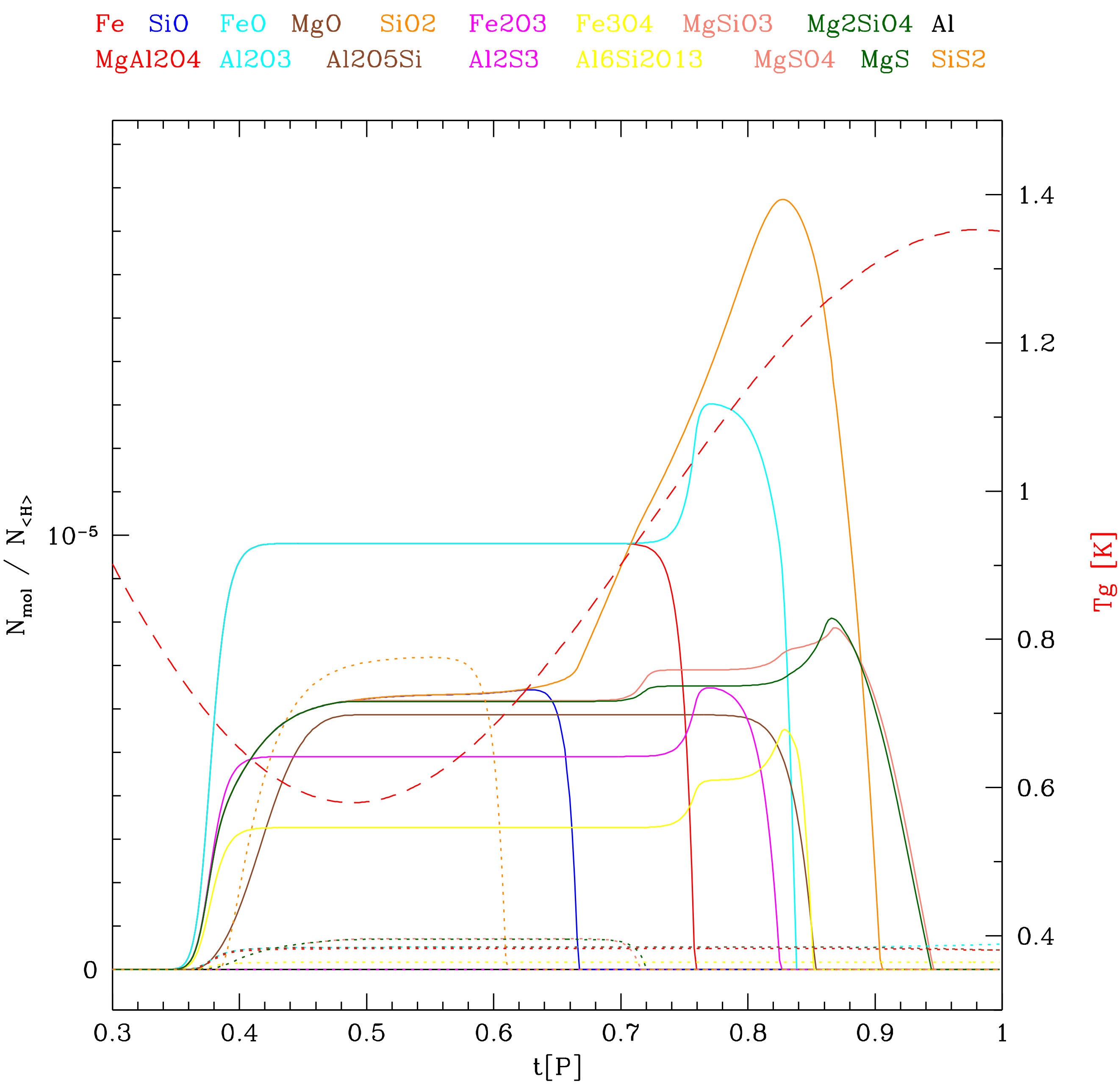

Figure 8: Molecular composition of the dust grains for **case B**